

existing as small clusters within these zones. Cluster formation would explain the preferential self-annihilation of lightly loaded  $\Delta, \Delta$ -Ru(bpy)<sub>3</sub><sup>2+</sup>\* at high-excitation flux. Coadsorbed Zn(phen)<sub>3</sub><sup>2+</sup> directs Ru(II) ions toward nonquenching sites and suppresses self-annihilation through pseudoracemic interaction with Ru(II). The distribution pattern of chelate ions changes with time on clay, the ions migrating toward nonquenching sites on hectorite and toward quenching sites on montmorillonite. That the binding modes of enantiomeric and racemic chelates differ on clay, and further that they may change with time, receives confirmation from light-scattering studies on flocculation behavior. Finally,

the deeper origins of binding state differences—with regard to both chirality and ligand type—must await a better understanding of host-guest interactions.

*Acknowledgment.* We thank Professor A. J. Bard for a preprint of ref 3 and Dr. V. Swayambunathan for helpful discussions. We also thank the Analytical Section, Alchemie Research Centre, and QC section, Fibres Division, ICI India Ltd., for assistance with analysis. This work was supported by the Office of Basic Energy Sciences of the Department of Energy, Bhabha Atomic Research Centre, and ICI India Ltd.

## Observation and Modeling of the Recombination Kinetics of Diphenylmethyl Radicals in the Cavities of Na-X Zeolite<sup>1</sup>

Linda J. Johnston,\* J. C. Scaiano,<sup>2a</sup> Ji-Liang Shi,<sup>2b</sup> Willem Siebrand, and Francesco Zerbetto<sup>2c</sup>

Steacie Institute for Molecular Sciences, National Research Council Canada, Ottawa, Ontario, Canada K1A 0R6 (Received: April 29, 1991)

An experimental and theoretical study is reported of the recombination of diphenylmethyl radicals generated from precursors included in Na-X zeolite. These precursors, 1,1,3,3-tetraphenylacetone and 1,1-diphenylacetone, are decomposed by flash photolysis, yielding a radical pair in a triplet configuration. The diphenylmethyl radical concentration, monitored by time-resolved diffuse reflectance spectroscopy, decreases roughly linearly with logarithmic time, indicative of a reaction rate that decreases gradually. The overall decay pattern depends only weakly on temperature, precursor, or laser dose. Product analysis indicates that geminate recombination, which requires a radical pair in a singlet configuration, is the dominant decay mechanism, consistent with the known mobility of diphenylmethyl radicals in the Na-X lattice. This face-centered lattice consists of large cavities each connected by channels to four other cavities situated at the corners of a tetrahedron. To describe the diffusion of the radicals in this lattice, a random walk model is adopted and solved by computer simulation. For short times (200 ns–10  $\mu$ s) and low precursor concentrations, the rate of geminate recombination generated by the model yields a satisfactory reproduction of the observed time dependence, but for long times the fraction of radicals surviving geminate recombination falls well below the theoretical limit of 51%. There is evidence that quenching processes other than nongeminate recombination are responsible for this behavior. It is found that the spin flip required to allow recombination is fast on the time scale of radical hopping and that the hopping rate of the order of  $10^6$ – $10^7$  s<sup>-1</sup> at room temperature is thermally activated with a substantial activation energy ( $\sim$ 2 kcal/mol in the range 244–327 K).

Recent experiments have shown that the kinetics of transients on surfaces or inside porous lattices may be very different from the first- and second-order processes governing most of solution chemistry.<sup>3–8</sup> A remarkable observation of our earlier exploratory studies on the behavior of diphenylmethyl radicals adsorbed on silica gel or included in the zeolites silicalite and Na-X was that the radical decay could be followed over at least 9 orders of magnitude in time, namely, from hundreds of nanoseconds to hours, indicative of a reaction rate that decreases gradually with

time.<sup>3</sup> In all these experiments the observed decay pattern over, say, 10 time units is nearly independent of the time unit chosen. Similar observations have been reported for several other radical pairs on various supports.<sup>8,9</sup>

These experiments make use of the technique of time-resolved diffuse reflectance spectroscopy, developed by Wilkinson and co-workers over the past decade,<sup>10–15</sup> which allows monitoring reaction intermediates supported by opaque media. Most of the supported transients studied to date are excited states of stable molecules.<sup>4–8,16–18</sup> The present extension of these studies to free

(1) Issued as NRCC 32855.

(2) Present address: (a) Department of Chemistry, University of Ottawa, Ottawa, Ontario, Canada K1N 6N5. (b) Shanghai Institute of Organic Chemistry, Academia Sinica, 345 Lingling Road, Shanghai, P. R. China. (c) Dipartimento di Chimica "G. Ciamician", Università di Bologna, Via F. Selmi 2, 40126 Bologna, Italy.

(3) Kelly, G.; Willsher, C. J.; Wilkinson, F.; Netto-Ferreira, J. C.; Olea, A.; Weir, D.; Johnston, L. J.; Scaiano, J. C. *Can. J. Chem.* **1990**, *68*, 812.

(4) Wilkinson, F.; Willsher, C. J.; Casal, H. L.; Johnston, L. J.; Scaiano, J. C. *Can. J. Chem.* **1986**, *64*, 539.

(5) Oelkrug, D.; Krabichler, G.; Honnen, W.; Wilkinson, F.; Willsher, C. *J. Phys. Chem.* **1988**, *92*, 3589.

(6) Oelkrug, D.; Uhl, S.; Wilkinson, F.; Willsher, C. *J. Phys. Chem.* **1989**, *93*, 4551.

(7) Draper, R. B.; Fox, M. A. *J. Phys. Chem.* **1990**, *94*, 4628.

(8) Kazanis, S.; Azarani, A.; Johnston, L. J. *J. Phys. Chem.* **1991**, *95*, 4430.

(9) Levin, P. P.; Ferreira, L. F. V.; Costa, S. M. B. *Chem. Phys. Lett.* **1990**, *173*, 277.

(10) Kessler, R. W.; Wilkinson, F. *J. Chem. Soc., Faraday Trans. 1* **1981**, *77*, 309.

(11) Kessler, R. W.; Krabichler, G.; Uhl, S.; Oelkrug, D.; Hagan, W. P.; Hyslop, J.; Wilkinson, F. *Opt. Acta* **1983**, *30*, 1099.

(12) Willsher, C. J. *J. Photochem.* **1985**, *28*, 229.

(13) Wilkinson, F.; Willsher, C. J. *Tetrahedron* **1987**, *43*, 1197.

(14) Oelkrug, D.; Honnen, W.; Wilkinson, F.; Willsher, C. J. *J. Chem. Soc., Faraday Trans. 2* **1987**, *83*, 2081.

(15) Wilkinson, F.; Kelly, G. In *Handbook of Organic Photochemistry*; Scaiano, J. C., Ed.; CRC Press: Boca Raton, FL, 1989; Vol. 1, Chapter 12.

(16) Turro, N. J.; Zimmt, M. B.; Gould, I. R. *J. Am. Chem. Soc.* **1985**, *107*, 5826.

(17) Turro, N. J.; Gould, I. R.; Zimmt, M. B.; Cheng, C.-C. *Chem. Phys. Lett.* **1985**, *119*, 484.

radicals seems timely in view of their role as key intermediates in many heterogeneous reactions, including several that are important in biology and in industry. The radical chosen for a detailed kinetic study is diphenylmethyl. It is generated directly inside the lattice of the zeolite Na-X whose large cavities (13 Å) will hold precursor molecules such as 1,1,3,3-tetraphenylacetone (TPA) or 1,1-diphenylacetone (DPA). Flash photolysis of either precursor leads to diphenylmethyl radicals which are small enough to move through the channels (8 Å) that connect the cavities in the chosen zeolite. Na-X is an aluminosilicate forming a face-centered cubic (fcc) lattice such that each cavity is linked to four other cavities situated at the corners of a tetrahedron. Hence, the linked cavities form a diamond structure. The radicals move through this lattice until they recombine or are scavenged.

The observed gradual decrease of the radical decay rate resembles the so-called stretched exponential decay observed for a wide variety of heterogeneous processes, including mechanical and dielectric relaxation, "hole burning" in absorption spectra, and free-radical reactions in glasses.<sup>19-31</sup> They are often represented as exponentials with fractional time exponents, i.e., in the form  $\exp(-ct^\beta)$  where  $\beta < 1$ . Some, but by no means all, of these processes can be described in terms of a distribution of first-order rate constants referring to a distribution of sites; this appears to be the case for hydrogen abstraction in rigid glasses.<sup>19,31-35</sup> However, this simple approach does not apply to our diphenylmethyl results since the recombination process must be second order. Other models that have been invoked generally involve collective behavior.<sup>25,29</sup> These also seem inappropriate for the dilute systems under consideration. The method we shall use to analyze the data is based on the random walk concept. It is suggested by the fact that the cavities form a regular, namely cubic, lattice, so that a diffusive mechanism based on random jumps to regularly spaced neighboring sites should be appropriate. Random walks in cubic lattices have been extensively studied,<sup>36</sup> mostly by polymer scientists. However, whereas for polymer studies, self-avoiding random walks are of particular relevance, a major complication in our model is the necessity of a spin flip before geminate recombination is possible, since the radical pairs are generated in a triplet configuration but recombine to yield a singlet state.

The experiments to be described involve variation of the precursor concentration, the laser intensity, and the temperature. We also study the effect of oxygen as a free-radical quencher and compare all results with the predictions of the random walk model.

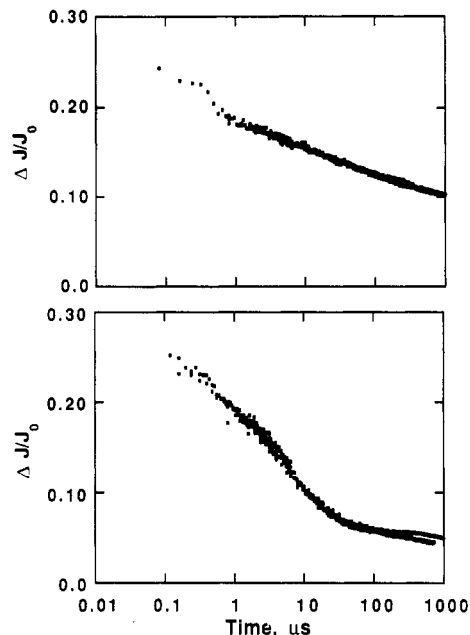


Figure 1. Decay of diphenylmethyl radical at 340 nm following 266-nm excitation of 3% TPA on Na-X under nitrogen (top) and oxygen (bottom).

### Experimental Section

**Materials.** 1,1,3,3-Tetraphenylacetone (TPA) was synthesized and purified according to a literature method.<sup>37,38</sup> 1,1-Diphenylacetone (DPA, Aldrich) was recrystallized before use. Na-X zeolite (BDH) was heated at 500 °C for 12 h and then stored in a desiccator.

**Sample Preparation.** Samples of either TPA or DPA on Na-X were prepared by stirring a hexane solution of the ketone with the zeolite (~2 mL/g) for 12 h and then slowly removing the solvent on a rotary evaporator. The sample was then vacuum-dried for 2 h at room temperature to remove final traces of solvent.

**Diffuse Reflectance Laser Flash Photolysis.** The experimental setup for diffuse reflectance has been described in detail elsewhere.<sup>8</sup> The fourth harmonic (266 nm; 10-ns pulses;  $\leq 25$  mJ/pulse) from a Lumonics Nd:YAG laser was used for sample excitation. Samples obtained in  $3 \times 7$  mm<sup>2</sup> quartz cuvettes were prepared by purging with nitrogen or oxygen for 30 min before the laser experiments. The data analysis is based on the fraction of reflected light absorbed by the intermediate ( $\Delta J/J_0$ ) where  $J_0$  is the signal before laser excitation and  $\Delta J$  is the difference between  $J_0$  and  $J_t$ , the signal at time  $t$  after laser excitation. Laser dose experiments show that increasing the laser intensity leads to an increase in signal intensity, demonstrating that a saturated plug of totally converted ground state to transient is not produced and that a Kubelka-Munk treatment of the data is not appropriate.<sup>14</sup>

**Product Studies.** Samples (0.5 g) of either TPA or DPA on Na-X, purged with nitrogen, were irradiated with 3000 laser pulses at 266 nm. The samples were shaken frequently to ensure uniform irradiation. After irradiation, the samples were extracted in a Soxhlet apparatus for 12 h using benzene as the solvent. The products were analyzed by GC (Perkin-Elmer 8320 gas chromatograph; 15 m  $\times$  0.242 mm DB-1 on fused silica capillary column) using biphenyl as the internal standard. GC/MS measurements were done on a Hewlett-Packard 5995 instrument equipped with a 10-m Ultra-1 (OV-101) capillary column.

### Laser Flash Photolysis Results

Excitation of samples containing 0.3–3 wt % TPA on Na-X produces strong signals with  $\lambda_{\text{max}}$  at 340 nm which have been assigned to the diphenylmethyl radical. The photolysis of TPA

(18) Drake, J. M.; Levitz, P.; Turro, N. J.; Nitsche, K. S.; Cassidy, K. F. *J. Phys. Chem.* **1988**, *92*, 4680.

(19) Siebrand, W.; Wildman, T. A. *Acc. Chem. Res.* **1986**, *19*, 238.

(20) Williams, G.; Watts, D. C. *Trans. Faraday Soc.* **1970**, *66*, 80.

(21) Zwanzig, R. J. *Chem. Phys.* **1965**, *43*, 714.

(22) Helfand, E. J. *Chem. Phys.* **1983**, *78*, 1931.

(23) Cohen, M. H.; Grest, G. S. *Phys. Rev. B* **1981**, *24*, 4091.

(24) Shlesinger, M. F.; Montroll, E. W. *Proc. Natl. Acad. Sci. U.S.A.* **1984**, *81*, 1280.

(25) Palmer, R. G.; Stein, D. L.; Abrahams, E.; Anderson, P. W. *Phys. Rev. Lett.* **1984**, *53*, 958.

(26) Jankowiak, R.; Richert, R.; Bäessler, H. *J. Chem. Phys.* **1985**, *89*, 4569.

(27) Richert, R.; Elschner, A.; Bäessler, H. *Z. Phys. Chem. (Munich)* **1986**, *149*, 63.

(28) Aubert, C.; Fünfschilling, I.; Zschokke-Gränacher, I.; Siebrand, W.; Wildman, T. A. *Chem. Phys. Lett.* **1985**, *122*, 465.

(29) Shlesinger, M. F. *Annu. Rev. Phys. Chem.* **1988**, *39*, 269.

(30) Alberty, W. J.; Bartlett, P. N.; Wilde, C. P.; Darwent, J. R. *J. Am. Chem. Soc.* **1985**, *107*, 1854.

(31) Doba, T.; Ingold, K. U.; Siebrand, W. *Chem. Phys. Lett.* **1983**, *103*, 339.

(32) Doba, T.; Ingold, K. U.; Siebrand, W.; Wildman, T. A. *Faraday Discuss. Chem. Soc.* **1984**, *78*, 175.

(33) Doba, T.; Ingold, K. U.; Siebrand, W.; Wildman, T. A. *J. Phys. Chem.* **1984**, *88*, 3165.

(34) Doba, T.; Ingold, K. U.; Siebrand, W. *Chem. Phys. Lett.* **1984**, *103*, 339.

(35) Doba, T.; Ingold, K. U.; Siebrand, W.; Wildman, T. A. *Chem. Phys. Lett.* **1985**, *115*, 51.

(36) Barber, M. N.; Ninham, B. W. *Random and Restricted Walks*; Gordon and Breach: New York, 1970.

(37) Dean, D. O.; Dickinson, W. B.; Quayle, O. R.; Lester, C. T. *J. Am. Chem. Soc.* **1950**, *72*, 1740.

(38) Scaiano, J. C.; Tanner, M.; Weir, D. *J. Am. Chem. Soc.* **1985**, *107*, 4396.

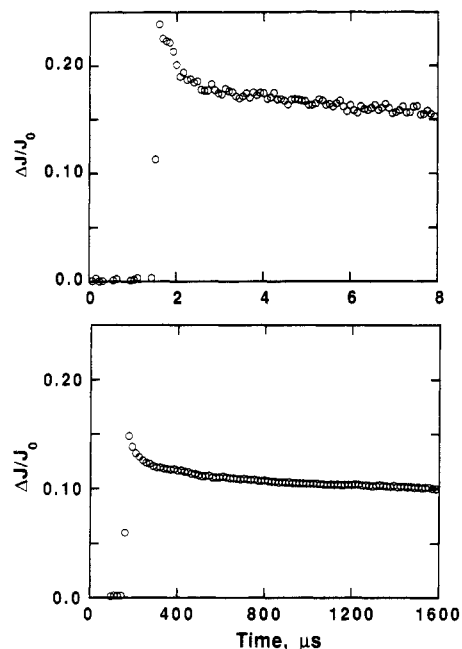


**Figure 2.** Transient decay at 340 nm for diphenylmethyl radical generated by 266-nm excitation of 3% TPA on Na-X. The two traces correspond to the beginning (top) and end (bottom) of the composite decay trace shown in Figure 1.

in solution produces a triplet diphenylmethyl radical pair within 10 ns since both  $\alpha$ -cleavage and loss of CO from the initial phenylacetyl radical occur rapidly (reaction 1).<sup>39</sup> As noted in  $\text{Ph}_2\text{CHC}(\text{O})\text{CHPh}_2 \rightarrow \text{Ph}_2\text{CHCO}^* + \text{Ph}_2\text{CH}^* \rightarrow 2\text{Ph}_2\text{CH}^* + \text{CO}$  (1)

our previous report, the decay of the diphenylmethyl radical signal on Na-X occurs over a wide range of time scales.<sup>3</sup> This is illustrated in Figure 1 (top) which shows a typical plot of signal intensity versus logarithmic time for a nitrogen-equilibrated sample. This particular trace was produced by measuring decay traces on a number of different time scales (two of these are plotted on a linear time scale in Figure 2) and then combining these into a single plot. It is usually necessary to normalize some of the traces in the region where they overlap in time, but these corrections are relatively small (<10%). In order to obtain reliable data for comparison with the modeling studies, it is essential to acquire data over as wide a range of time scales as possible. In practice, our first reliable data point could only be recorded  $\sim 250$  ns after the laser pulse. Our time resolution is limited by the presence of a relatively strong luminescence (at our monitoring wavelength of 340 nm at short delays) for which complete correction is difficult and by the fact that laser excitation of TPA is known to generate excited diphenylmethyl radicals which have a lifetime of  $\sim 150$  ns based on luminescence measurements (at 520 nm) on this zeolite. At long time scales our experiments are limited to  $\sim 800$   $\mu\text{s}$  by the stability and duration of the pulse from the monitoring beam.

Data for the decay of the diphenylmethyl radical were measured over our entire range of accessible time scales under a variety of conditions. These included variation of the temperature from 54 to  $-30$   $^\circ\text{C}$ , variation of the laser dose by a factor of  $\sim 6$ , and variation of sample loading (0.3–3%). The decay of the diphenylmethyl radical for a 3% sample under a nitrogen atmosphere was measured a number of times to check for reproducibility. In all cases the traces obtained were similar to that shown in Figure 1 (top); there was always a substantial fraction of radicals that persisted for long times ( $>100$   $\mu\text{s}$ ), although the amount varied slightly from one experiment to the next. As shown in Figure 3, temperature had little effect on the shape of the decay traces or

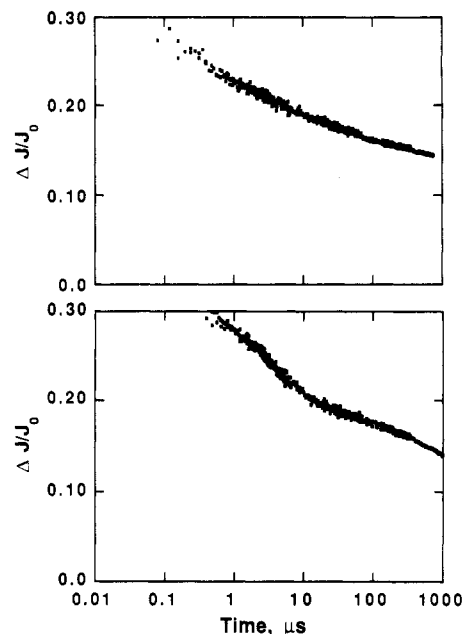


**Figure 3.** Decay of diphenylmethyl radical at 340 nm for 3% TPA on Na-X at 327 K (top) and 244 K (bottom).

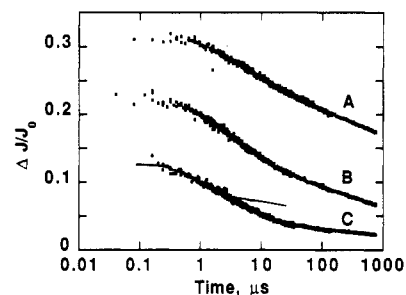


**Figure 4.** Decay of diphenylmethyl radical at 340 nm for 3% (A) and 0.3% (B) TPA on Na-X at high laser dose and for 0.3% TPA (C) at low laser dose. The line through (C) represents the calculated curve for geminate recombination.

the amount of residual, at least over the range 54 to  $-30$   $^\circ\text{C}$ . However, the overall decay is faster at the higher temperature as can be readily seen if the two curves are superimposed: the high-temperature curve appears to be shifted to shorter times relative to the low-temperature curve, which suggests that the site-to-site hopping is thermally activated. As shown in Figure 4, decreasing the laser dose reduced the overall signal intensity, although, as observed previously,<sup>3</sup> the effects were not linear with laser intensity. However, the shapes of the decay traces were very similar at various laser doses, except for the fact that there was a slightly smaller fraction of radicals which had not decayed after 1 ms at the lower doses. The initial flat portion of the high-dose decay curve is probably an artifact due to incomplete correction for extraneous effects, including the formation of excited radicals with a lifetime of about 150 ns. For these reasons, points measured at times shorter than 300 ns are not regarded as accurate.

Differences in sample loading had a somewhat stronger effect on the shape of the decay curve. Although the curves in Figure 4, corresponding to two samples with a 10-fold difference in loading (3% vs 0.3%), appear to run parallel, the fractional decrease per unit  $\log t$  is initially much faster for the lower load sample which also is left with a much smaller fraction of surviving radicals at the end of the experiment (1 ms).

In addition to these results, there were pronounced effects when the samples were equilibrated with oxygen rather than nitrogen prior to measurement of the decay traces. Figure 1 (bottom) shows a plot of signal intensity vs  $\log t$  for an oxygenated sample. In this case a substantial fraction of the radicals decays more rapidly than for a similar sample under nitrogen. However, there are some radicals which are obviously very well protected from

(39) Gould, I. R.; Baretz, B. H.; Turro, N. J. *J. Phys. Chem.* **1987**, *91*, 925.

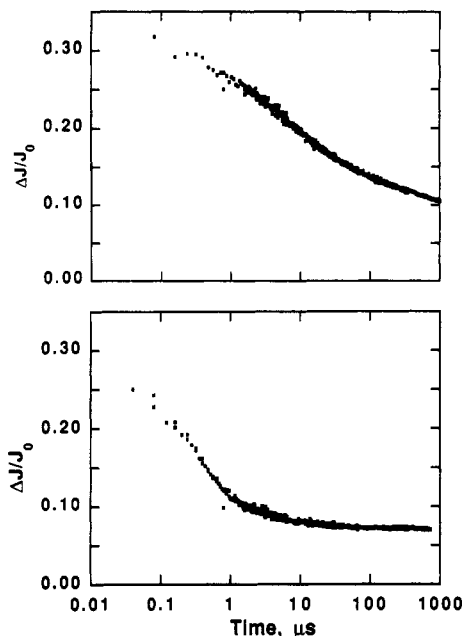


**Figure 5.** Decay of diphenylmethyl radical at 340 nm for 3% DPA on Na-X under nitrogen (top) and oxygen (bottom).

oxygen since after  $\sim 100 \mu\text{s}$  the signal levels off, even though 10–20% of the initial radicals are still present. Previous results have demonstrated that the spectrum of the remaining radicals is unchanged even over a period of minutes following laser excitation.<sup>3</sup>

Diphenylmethyl radicals can also be generated by photolysis of 1,1-diphenylacetone (reaction 2) which yields a triplet di-



phenylmethyl/acetyl radical pair. Decay traces (Figure 5) from this precursor (at 3.3% sample loading) were similar to those recorded using 3% TPA as the radical source. Again, the decay of the radical was relatively insensitive to temperature and laser intensity. Under oxygen the radicals decayed more rapidly; in this case the decay traces leveled off to a constant residual absorption more quickly than for the TPA samples.

Product analyses were carried out for several of the samples used in the time-resolved experiments. Samples of TPA and DPA equilibrated with either nitrogen or oxygen were irradiated with 3000 laser shots, and the products were extracted and analyzed as outlined in the Experimental Section. Irradiation of TPA on Na-X under nitrogen gave 1,1,2,2-tetraphenylethane and small amounts of diphenylmethane (10–20%); in contrast, for an oxygenated sample, benzophenone and five other unidentified products were detected by GC, in addition to tetraphenylethane and diphenylmethane. Irradiated samples of DPA did not show any trace of tetraphenylethane, indicating that nongeminate recombination of the radical pair does not contribute significantly to the decay of the diphenylmethyl radical in this system.

**Geminate Recombination Kinetics.** To model the kinetics of the diphenylmethyl radicals, we assume that the radicals perform random walks. Optical excitation of TPA generates a pair of these radicals in a triplet configuration within the cavity where the TPA molecule is located. Once formed, the radicals have two options: either they can recombine, which requires a spin flip, or at least one of them can escape to an adjacent cavity through one of the four available channels. To be specific, we associate time constants  $\theta$  and  $\tau$  with these two processes, respectively. Since their relative magnitudes are not known a priori, both parameters must be retained in the model. It will be instructive, however, to consider first the two special cases where one parameter dominates.

In the limit  $\theta \ll \tau$ , most of the radical pairs formed initially will recombine before leaving their cavity. Our detection system can only observe radicals surviving for times longer than about 200 ns, which implies that the observed signal will be due to radical pairs having separated into different cavities. If on their walk

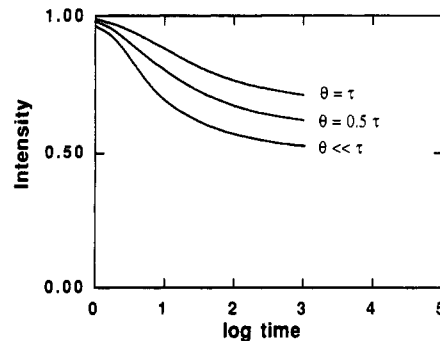


**Figure 6.** Calculated decay curves for geminate recombination in the limit  $\theta \ll \tau$  and under conditions where  $\theta$  and  $\tau$  are of comparable magnitude.

through the lattice two radicals meet in the same cavity, they will recombine with a high probability, irrespective of their spin. Thus, to calculate the rate of decay of the radical concentration in this limit, we need only consider the rate at which two radicals meet. Since for short times these two radicals are likely to be the geminate pair initially generated, this procedure is very similar to the standard problem of a single random walker returning to its point of origin. The similarity is due to the fact that in our example it makes no difference how the two radicals share the jumps. Obviously, if only one of them jumps, the problem reduces to that of a single walker.

Random walks on a diamond lattice have been discussed before.<sup>36</sup> However, our lattice differs from the standard diamond (fcc) lattice in that the number of accessible neighbors is four rather than 12, namely determined by the channels linking the cavities. Therefore, the analytical techniques used to treat random walks on an fcc lattice cannot be immediately generalized to our lattice, as briefly discussed in Appendix A.

However, the random walk can be readily simulated by computer modeling. In our model the radicals start from adjacent sites in the fcc lattice, say (000) and (101), and can reach one out of four neighboring sites in one jump; e.g., the radical at (000) can jump to ( $\pm 101$ ) or ( $0\pm 1-1$ ). They will jump at random to one of these sites, the probability of a jump at time  $t$  being given by  $\exp(-t/\tau)$ . The random jumps to adjacent sites are repeated until the two radicals meet in the same cavity or until they are separated by a given distance, chosen to be so large that subsequent encounters are extremely improbable. In the program the lattice is infinite. The simulation showed that the average separation between two geminate radicals is given by the square root of the number of jumps. Although the fate of some pairs was pursued for more than  $10^5$  jumps, leading to an average separation of  $10^{2.5}$  sites, it was found that after  $10^3$  jumps subsequent encounters were essentially negligible. To accumulate reliable statistics, more than  $10^6$  pairs were followed for up to  $10^3$  jumps. The results are depicted in Figure 6 (lowest curve) in the form of a decay curve plotted on a logarithmic time scale. It shows how fast the radicals decay by geminate recombination if each encounter leads to reaction.

In an infinite lattice, not all pairs meet again: about half, namely 51%, escape recombination. In a standard fcc lattice with 12 rather than four nearest neighbors, this number increases to 74%.<sup>36</sup> The escape probability can be written in the form

$$f = 1 - \sum_{n(\text{odd})}^{\infty} a_n \quad (3)$$

where  $a_n$  is the probability that the  $n$ th jump leads to recombination. By symmetry,  $a_n = 0$  if  $n$  is even for the present lattice. Clearly,  $a_1 = 1/4$  in our case and  $1/12$  for the standard fcc lattice. For two-dimensional lattices, e.g., a square lattice (four nearest neighbors) or a graphite-like lattice (three nearest neighbors),  $f = 0$ ; i.e., all radical pairs will ultimately recombine.

We now consider the opposite limit,  $\theta \gg \tau$ , where essentially all radical pairs initially created separate into different cavities. Their disappearance by geminate recombination will be subject to a factor  $\exp(-\theta/t)$  which will be substantially different from

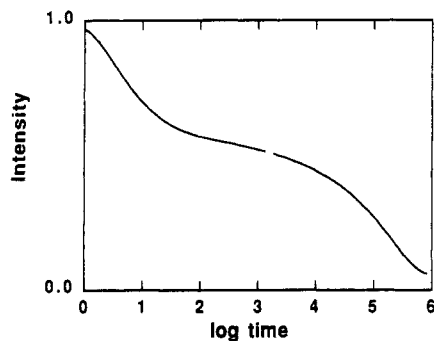


**Figure 7.** Calculated decay curves for geminate (0–3 log time units) and nongeminate (3–6 log time units) recombination.

zero only for times long compared to  $\tau$ , so that on average the pairs will have drifted far apart before any meeting can lead to recombination. Thus, in this case the escape probability will be close to unity and the radical decay curve will be essentially flat until nongeminate recombination takes over.

In the general case where  $\theta$  and  $\tau$  are of comparable magnitude, we expect intermediate behavior, leading to decay curves that interpolate between the two limiting curves. Since the probability that a triplet encounter pair will recombine is  $\exp(-\theta/\tau)$ , multiplication of the separation of the two limiting curves by this factor should produce a reasonable interpolation. A more accurate method of deriving intermediate curves is discussed in Appendix B. The resulting curves for  $\theta/\tau = 0.5$  and 1 are also illustrated in Figure 6. Compared to the "standard" curve, obtained for  $\theta = 0$ , the new curves are flatter, indicating a slower decay of the radical concentration and a larger survival probability.

**Nongeminate Recombination Kinetics.** A radical escaping geminate recombination is still subject to nongeminate recombination since the originally nonuniform radical distribution will evolve toward uniformity in a time governed by the average separation of the newly created radical pairs at the start of the experiment. This average separation can be deduced from the initial concentration of radical pairs if that concentration is uniform. Since a fraction  $f$  of the radicals escapes geminate recombination, the fraction of radicals subject to nongeminate recombination at  $t = 0$  equals  $2f$  times the concentration of radical pairs at  $t = 0$ .

Thus from  $t = 0$ , the radicals are subject to two recombination processes: geminate, described above, and nongeminate, described by the standard rate equation

$$x(t) = \frac{2fc}{1 + 2fck_2t} \quad (4)$$

where  $c$  is the original radical-pair concentration, which for simplicity we set equal to the average number of pairs per grain, assuming an approximately uniform grain size. The nongeminate second-order rate constant is given by

$$k_2 = 8\pi gDR \quad (5)$$

$D$  being the diffusion constant,  $R$  the reaction radius, and  $g$  the probability that the two radicals are in or transfer into a singlet configuration during the encounter. Since at unit jump distance the probability of recombination is  $g/4$ , we write  $R = 1/4$  so that  $k_2 = 2\pi gD = \pi g/3\tau$ . To estimate  $g$ , we note that we cannot simply set  $g = p$ , defined by eq B1, because of the possibility of multiple encounters. If nongeminate recombination becomes significant only after geminate recombination is virtually complete, these multiple encounters will be effective only during a time that is very short on the time scale of the nongeminate process. We can then set  $g = 1 - f$ , so that

$$x(t) = \frac{6fc\tau}{3\tau + 2\pi f(1-f)ct} \approx \frac{2fc}{1 + 2f(1-f)ct/\tau} \quad (6)$$

The shape of this curve, plotted in Figure 7 against  $\log t$ , is robust; i.e., a change in parameter values will only lead to a shift along the  $\log t$  scale and/or a rescaling of the vertical axis. It is readily

seen that the maximum slope corresponding to the inflection point  $t = t_i$  of the  $dx/d(\log t)$  curve equals  $-2.303fc/2$  for  $t_i = \tau/2f(1-f)c$ . Thus, if the concentration changes from  $c_1$  to  $c_2$ ,  $dx/d(\log t)$  rescales linearly with  $c$  and  $\log t_i$  shifts by  $\log(c_1/c_2)$ .

Since we assume geminate recombination to be virtually complete when nongeminate recombination becomes significant, we can combine the geminate and nongeminate decay curves by setting the number of radicals at the end of the geminate process equal to  $2fc$ . The maximum slope associated with this process occurs for short times ( $t \approx \tau$ ); from Figure 6 and Appendix B, we obtain

$$\left[ \frac{dx}{d \log t} \right]_{\tau} \approx - \frac{1 - (1 - p_1/4)}{0.77} 2c = -0.65cp_1 \quad (7)$$

which is to be compared to the maximum slope for the nongeminate process

$$\left[ \frac{dx}{d \log t} \right]_{t_i} = -1.15fc \quad (8)$$

derived above. For  $\theta/\tau = 0, 0.5$ , and 1, we have respectively  $[dx/d \log t]_{\tau}/[dx/d \log t]_{t_i} = 1.1, 0.56$ , and 0.29. These two downward-sloping sections of the  $\log t$  plot are separated by a section with a very small slope (Figure 7). This section will shrink if the concentration of radicals is increased, leading presumably to a smooth merger of the two sloping sections for sufficiently high radical concentrations.

In the case of the DPA precursor, where the two combining radicals can be different, the fact that their diffusion coefficients are not the same will complicate the calculation slightly. A more serious complication arises if oxygen is present. The oxygen concentration will generally be different from the radical concentration and presumably much larger. Since the reaction between the radicals and oxygen does not require a spin flip, we may formally set  $\theta = 0$ , so that the standard second-order decay law will take the form

$$\frac{x}{2c} = \frac{b - 2c}{b \exp[(b - 2c)k_2t] - 2c} \quad (9)$$

where  $b$  is the oxygen concentration and  $c$  the initial radical-pair concentration. This mechanism should be competitive with geminate recombination. For  $b \gg 2c$ , the rate law becomes effectively first order

$$x = 2c \exp(-bk_2t) \quad (10)$$

producing an extremely steep decay curve on a  $\log t$  scale.

## Discussion

Before comparing the observed properties of the system with the random walk model of the preceding section, we note that the observed nonexponential time dependence resembles the "stretched" exponential dependences observed for a wide variety of processes.<sup>19-31</sup> Many models have been proposed for these observations, the simplest of which leads to a distribution of first-order rate constants.<sup>19,26-28,30,31</sup> In the present case, where the reaction eliminating the radicals is second-order, this would require generalization to a distribution of second-order rate constants. However, no physically acceptable distribution has been found that would reproduce the observed decay rate. The same applies to distributions of first-order rate constants, based on the assumption that a first-order process such as triplet-to-singlet conversion in the radical pair is rate-determining. In both instances, the distributions required are far too broad to be credible. Other models, involving collective effects,<sup>25,29</sup> are unlikely to apply in our system where interaction between radicals in different cavities will be extremely weak.

By contrast, the random walk model of radical recombination has an inherent plausibility since species of the size of the radicals and their precursors are known to be mobile in the zeolite used and the product analysis is consistent with (geminate) recombination being a leading mechanism of radical decay. Random walk

is simply a diffusion process constrained by the topology of the lattice, which, in our case, consists of a regular array of cavities, each of which is connected to four adjacent cavities by means of channels. This model predicts that the initial rate of radical decay is an approximately linear function of logarithmic time, as observed. The slope  $dc/d \log t$  is governed by the lattice topology, in agreement with the observation that this slope shows no strong dependence on temperature, laser dose, or type of precursor used. However, there is a clear dependence on the precursor loading: a 10-fold increase in load increases the initial radical signal by a factor of less than 2 and causes a slowing down of the decay.

First, we consider the low-load, low-dose curve (c in Figure 4); its initial slope, up to about 20  $\mu$ s, is close to that predicted by the random walk model for  $\theta \ll \tau$ . However, whereas the random walk model leads to  $f = 0.51$ , the fraction surviving after 1 ms is actually less than 0.2. There are several indications that the additional decay is not due to nongeminate recombination. First, in the case of the DPA precursor, a much higher concentration of radicals yields no measurable amount of tetraphenylethane, which would be one of the principal nongeminate reaction products. Second, for higher concentrations of radicals, nongeminate recombination would become important at earlier times, but no such effect is apparent when the load is increased. On the contrary, increasing the precursor load actually decreases the slope while the fraction surviving at 1 ms increases to about 0.5. Note that, in the high-dose experiments, data points for  $t < 300$  ns should be discarded, since the laser generates excited radicals with a lifetime of about 150 ns whose absorption remains undetected during this time.

If the additional decay process is not nongeminate recombination, it may be radical quenching by impurities or active sites in the lattice or it may be a surface effect. If radicals are reflected back into the bulk when reaching the surface, the fraction escaping recombination will obviously be reduced. An even stronger reduction may be expected if, instead, these radicals continue to move along the surface, because of the reduced dimensionality of this random walk situation.

However, there is an alternative interpretation, based on the observation that the curves in Figure 4 appear to be nearly parallel. This suggests that the "divergence" of these curves is a baseline effect, indicative of the presence of unreactive radicals. That there are such radicals, at least in the high-load samples, is demonstrated by the fact that oxygen quenches only part of the radicals. If we use the surviving fraction as a baseline correction, the difference in initial slope between the high-dose, high-load sample and the low-dose, low-load sample all but vanishes.

These unreactive radicals may be trapped in cavities containing a precursor molecule. This interpretation is based on the assumption that interaction with the precursor will lead to the formation of a relatively stable complex which energetically or sterically protects the radical against oxygen and other radicals. Some support for this interpretation can be derived from the different effect of oxygen on radicals formed from TPA and DPA. The two plots (Figures 1 and 5, bottom) have the same overall shape but differ along the  $\log t$  scale by about 1 unit, indicating that the radicals generated from DPA disappear 10 times as fast as those generated from TPA. Since the radicals are the same, this must be a precursor effect, probably due to the fact that DPA is smaller than TPA and hence less effective in protecting the radical against reaction with oxygen.

Accepting tentatively that, after this baseline correction, the decay curves of the high-dose, high-load samples reflect mostly bulk recombination, we can evaluate the effect of temperature displayed in Figure 3. The principal effect of increasing the temperature from 244 to 327 K is a shift of about  $-\log 3$  along the  $\log t$  axis, which suggests that the temperature increase decreases the residence time by a factor of 3. If  $\tau^{-1}$  follows the Arrhenius equation, this implies an activation energy for radical hopping of about 700  $\text{cm}^{-1} \approx 2$  kcal/mol. The actual hopping time can be roughly estimated from a comparison of Figure 4 with the theoretical curves of Figure 6. A good fit is obtained for  $\theta \gg \tau \sim 300$  ns at room temperature; in the absence of reliable

data for  $t < 300$  ns, the uncertainty of this number is estimated to be a factor of 2.

Comparison of the decay curves of radicals generated from TPA and DPA, depicted in Figures 1 and 5, respectively, indicates that the latter lies to the left of the former, indicating a slightly shorter residence time  $\tau$  for the DPA sample. This effect can be easily explained in terms of the smaller size of the acetyl radical relative to the diphenylmethyl radical, leading to faster hopping of acetyl.

Obviously our experiments depend on many variables, not all of which are easy to control. In view of the complexity of the system, the amount of data collected thus far remains very limited. In spite of these limitations, a reasonably consistent picture can be tentatively drawn of the fate of a radical pair photogenerated in a Na-X zeolite cavity. It has a much better chance to recombine than to separate into adjacent cavities. Once separated, geminate recombination rather than spin relaxation controls the survival. Theory predicts that after ca.  $10^2$  hops the radicals should be essentially stable until nongeminate processes take over (see Figure 7). However, our experimental data show that radical decay, though slow, continues after 10  $\mu$ s. This suggests that when the geminate process essentially shuts off, other mechanisms or radical scavenging processes take over. The apparent absence of nongeminate recombination sets an upper limit to the range of the radicals: it must be smaller than the average separation between different radical pairs at the start of the experiment, i.e., smaller than about 20 lattice spacings (based on an estimated concentration of one radical per  $10^4$  cavities). A substantial fraction of the radicals gets trapped at sites where they are protected from recombination and quenching, even in the presence of oxygen. These sites may be cavities containing precursor molecules. Since the precursor concentration is much higher than the radical pair concentration, such trapping would have a much higher probability than nongeminate recombination.

This scenario opens interesting possibilities for the control of chemical reactions inside zeolites, based on radicals that survive for long periods of time and remain mobile. However, the region of the lattice that the radicals explore before being subjected to scavenging remains quite limited in our experiments, which may indicate a need for better control of the sample preparation.

*Acknowledgment.* We thank Mr. S. Sugamori and Mr. G. Charette for technical assistance.

## Appendix A

The question arises whether some of the properties of the present random walk model can be handled algebraically. For instance, for standard cubic lattices, it is possible to derive closed-form expressions for the probability that a random walker will not return to the point of origin. As argued in the main text, this is equivalent in our model to the probability that a geminate pair of walkers will not meet again. According to standard random walk theory,<sup>36</sup> this probability is given by  $U^{-1}$ , where

$$U = \frac{1}{8\pi^3} \int_{-\pi}^{\pi} \int_{-\pi}^{\pi} \int_{-\pi}^{\pi} \frac{d\phi_1 d\phi_2 d\phi_3}{1 - \lambda(\phi)} \quad (\text{A1})$$

The  $\phi_i$  in this integral are reciprocal lattice vectors,  $\phi = \{\phi_1, \phi_2, \phi_3\}$  and  $\lambda(\phi)$ , the structure factor of the walk, is the Fourier transform of the probability distribution  $p(\mathbf{r})$  of steps  $\mathbf{r}$ :

$$\lambda(\phi) = \int_{-\infty}^{\infty} p(\mathbf{r}) \exp(i\phi\mathbf{r}) d\mathbf{r} \quad (\text{A2})$$

In the case at hand, we assume equal probability for single steps to neighboring sites and zero probability for all other steps.

The diamond lattice is an fcc lattice where each site has 12 nearest neighbors. The corresponding structure factor is

$$\lambda(\phi) = (1/3)(\cos u \cos v + \cos v \cos w + \cos w \cos u) \quad (\text{A3})$$

where  $u$ ,  $v$ , and  $w$  are directions in the reciprocal lattice. The corresponding 12 displacements are given by vectors  $(\pm 1, \pm 1, 0)$ ,  $(\pm 1, 0, \pm 1)$ , and  $(0, \pm 1, \pm 1)$ . However, in our case only four of these displacements are allowed, namely  $(\pm 1, 0, 1)$  and  $(0, \pm 1, -1)$  or their

cyclic permutations. The corresponding structure factor

$$\lambda(\phi) = (1/2)[\cos u \exp(iw) + \cos v \exp(-iw)] \quad (\text{A4})$$

leads to the integral

$$U = \frac{16}{\pi^3} \int_0^{\pi/2} \int_0^{\pi/2} \int_0^{\pi/2} \frac{du \, dv \, dw}{2 - \cos u \exp(iw) - \cos v \exp(-iw)} \quad (\text{A5})$$

which so far has successfully resisted analytical solution. We note, however, that the integral obtained if  $\lambda(\phi)$  is replaced by

$$\text{Re } \lambda(\phi) = (\cos u + \cos v) \cos w \quad (\text{A6})$$

can be handled effectively by the method of Watson.<sup>40</sup> Thus transformation to Cartesian coordinates  $x = \tan(1/2u)$ ,  $y = \tan(1/2v)$ , and  $z = \tan(1/2w)$  followed by transformation to polar coordinates  $x = r \sin \theta \cos \psi$ ,  $y = r \sin \theta \sin \psi$ , and  $z = r \cos \theta$ , leads to

$$U = \frac{2}{\pi^3} \int_0^{\pi/2} \int_0^{\pi/2} \int_0^{\infty} dr \, d\theta \, d\psi \times \sin \theta / [1 + \cos^2 \theta + r^2 \sin^2 \theta (\cos^2 \theta + 1/2 \sin^2 \theta \sin^2 \psi)] \quad (\text{A7})$$

where  $\psi = 2\phi$ . The integration over  $z$  can be carried out at once

$$U = \frac{2}{\pi^2} \int_0^{\pi/2} \int_0^{\pi/2} \frac{d\theta \, d\psi}{[(1 + \cos^2 \theta)(\cos^2 \theta + 1/2 \sin^2 \theta \sin^2 \psi)]^{1/2}} \\ = \frac{2}{\pi^2} \int_0^{\pi/2} \int_0^{\infty} \frac{d\tau \, d\psi}{[(1 + \tau^2)(1 + \tau^2 \sin^2 \psi)]^{1/2}} \quad (\text{A8})$$

where  $\tau = 2^{-1/2} \tan \theta$ . The integral over  $\tau$  is a complete elliptic integral of the first kind and should be solvable by Watson's method.<sup>36,40</sup>

However, eq A6 corresponds to displacement vectors  $(\pm 1, 0, \pm 1)$  and  $(0, \pm 1, \pm 1)$ , i.e., an fcc lattice with eight rather than four nearest neighbors. Hence, it does not apply directly to our lattice. If the same transformations are applied to the integral (A4), the denominator of the integral contains terms in  $r$  as well as  $r^2$  so that direct integration is not possible.

It is readily seen that reduction to a two-dimensional lattice, e.g., a square lattice with four nearest neighbors or a graphite lattice with three nearest neighbors, leads to divergent integrals, i.e.,  $U^{-1} = 0$ , indicating that in such a lattice all radicals will ultimately recombine.

### Appendix B

The effect of a spin-relaxation time  $\theta$  of the same order as the hopping time  $\tau$  on the radical decay curve of Figure 6 can be

(40) Watson, G. N. *Q. J. Math* 1939, 10, 266.

evaluated analytically. For short times the spin-memory function  $\exp(-\theta/t)$  will control recombination, and for long times spin statistics, favoring triplet over singlet encounters by a factor of 3, will be the limiting factor. The probability that a triplet encounter will lead to recombination is clearly  $\exp(-\theta/t)$ . When two radicals meet at time  $t$ , the overall probability of recombination is thus

$$p(t) = [3 \exp(-\theta/\tau) + \exp(-\theta/t)]/4 \quad (\text{B1})$$

Similarly, the probability that a pair meeting after  $n$  jumps will recombine is

$$p_n = [3 \exp(-\theta/\tau) + \exp(-\theta/n\tau)]/4 \quad (\text{B2})$$

To calculate the escape probability, we must take into account that pairs may have multiple encounters. Each encounter not leading to recombination generates a pair of radicals in a triplet configuration at adjacent sites; i.e., it regenerates the original geminate pair. The resulting escape probability can be expressed in the form of a geometric series

$$f = 1 - \sum_n p_n a_n \{1 + \sum_n (1 - p_n) a_n + [\sum_n (1 - p_n) a_n]^2 + \dots\} \\ = 1 - \frac{\sum_n p_n a_n}{1 - \sum_n (1 - p_n) a_n} \\ = \frac{1 - \sum_n a_n}{1 - \sum_n a_n + \sum_n p_n a_n} = \frac{1}{1 + 1.96 \sum_n p_n a_n} \quad (\text{B3})$$

where we have used the value  $\sum_n a_n = 0.49$  obtained from the computer model.

Experimentally, one observes a quantity  $f(t)$ , the fraction of the radicals surviving at time  $t$ , which in the model takes the form  $f(N)$ , the fraction surviving  $N$  jumps:

$$f(N) = 1 - p_1 a_1 \{1 + (1 - p_1) a_1 + [(1 - p_1) a_1]^2 + \dots + [(1 - p_1) a_1]^{N-2} + (1 - p_3) a_3 + \dots + [(1 - p_3) a_3]^{N-4} + 2(1 - p_1) a_1 (1 - p_3) a_3 + \dots + [2(1 - p_1) a_1 (1 - p_3) a_3]^{N-6} + \dots\} - p_3 a_3 \{1 + (1 - p_1) a_1 + \dots + [(1 - p_1) a_1]^{N-4} + \dots\} \dots p_N a_N \\ = 1 - \sum_n p_n a_n \{1 + \sum_m^{N-n-1} (1 - p_m) a_m + [\sum_m^{N-n-3} (1 - p_m) a_m]^2 + \dots\} \\ = 1 - \sum_n p_n a_n \{1 + \sum_{j=1}^{1/2(N-1)} [\sum_m^{N-n-j} (1 - p_m) a_m]^j\} \quad (\text{B4})$$

with both  $m$  and  $n$  (but not  $j$ ) odd. In the limit  $N \rightarrow \infty$ , eq B4 clearly reduces to eq B3. For  $\theta \rightarrow 0$  and thus  $p \rightarrow 1$ , reduction to the standard random walk model is obtained; for  $\theta/\tau \rightarrow \infty$  and thus  $p \rightarrow 0$ , we have  $f \rightarrow 1$ , i.e., no recombination.